Published in final edited form as:
Clin Transl Oncol. 2008 November ; 10(11): 726–738. doi:10.1007/s12094-008-0279-5.

Identification of the Rock-dependent transcriptome in rodent fibroblasts

Inmaculada M. Berenjeno and **Xosé R. Bustelo**
Centro de Investigación del Cáncer and Instituto de Biología, Moleculary Celular del Cáncer (IBMCC), CSIC – University of Salamanca, Campus Unamuno, ES-37007 Salamanca, Spain

Inmaculada M. Berenjeno: ; Xosé R. Bustelo: xbustelo@usal.es

Abstract

Rock proteins are Rho GTPase-dependent serine/threonine kinases with crucial roles in F-actin dynamics and cell transformation. By analogy with other protein kinase families, it can be assumed that Rock proteins act, at least in part, through the regulation of gene expression events. However, with the exception of some singular transcriptional targets recently identified, the actual impact of these kinases on the overall cell transcriptome remains unknown. To address this issue, we have used a microarray approach to compare the transcriptomes of exponentially growing NIH3T3 cells that had been untreated or treated with Y27632, a well known specific inhibitor for Rock kinase activity. We show here that the Rock pathway promotes a weak impact on the fibroblast transcriptome, since its inhibition only results in changes in the expression of 2.3% of all the genes surveyed in the microarrays. Most Y27632-dependent genes are downregulated at moderate levels, indicating that the Rock pathway predominantly induces the upregulation of transcriptionally active genes. Although functionally diverse, a common functional leitmotiv of Y27632-dependent genes is the implication of their protein products in cytoskeletal-dependent processes. Taken together, these results indicate that Rock proteins can modify cytoskeletal dynamics by acting at post-transcriptional and transcriptional levels. In addition, they suggest that the main target of these serine/threonine kinases is the phosphoproteome and not the transcriptome.

Keywords

Rock; Rho/Rac GTPases; Microarray; Gene expression; Transcription; Cytoskeleton

Introduction

The Rho/Rac family is a large group of GTP-binding proteins specialised in the regulation of a wide spectrum of cellular functions such as cytoskeletal organisation, cell proliferation, vesicle trafficking and cytokinesis [1–6]. Rho/Rac proteins are regulated by extracellular stimulus-dependent changes in their bound guanosine nucleotides. In non-stimulated cells, these proteins are bound to GDP molecules and in an inactive conformation [1,7]. In addition, they remain sequestered in the cytosol due to their interaction with Rho GDP dissociation inhibitors (RhoGDIs) [1,8,9]. In stimulated cells, these proteins are released from RhoGDIs, translocate from the cytosol to cellular membranes and undergo the exchange of GDP by GTP. This exchange of nucleotides promotes a conformational change in the GTPase switch regions that, in turn, allows the binding of downstream effectors [1]. This activation step, as well as

Correspondence to: Xosé R. Bustelo, xbustelo@usal.es.

The genomic data of this work are deposited in the NCBI Gene Expression Omnibus database (Accession number: GSE5913).

its subsequent inactivation by hydrolysis of the bound GTP molecules, is catalysed by guanosine nucleotide exchange factors and GTPase activating proteins, respectively [10,11]. According to structural criteria, Rho/Rac proteins can be subdivided in Rho (RhoA, RhoB, RhoC), Rac (Rac1, Rac2, Rac3, RhoG) and Cdc42 (Cdc42, TTF) subfamilies [1]. Within the Rho subfamily, RhoA is perhaps the best characterised in terms of three-dimensional structure, effectors and its participation in normal and pathological-related biological responses [1,12–15].

The elucidation of the regulation and function of RhoA effectors is important to understanding the intracellular pathways that control RhoA-dependent cellular, physiological and pathological responses. Two of the main RhoA effectors are the highly related serine/threonine kinases RockI (also known as Rokβ and $p160^{Rock}$) and RockII (also referred to as both Rokα and Rho kinase) [16,17]. These proteins become activated during signal transduction by the binding to Rho subfamily members [16,17] and/or second messengers such as arachidonic acid [18] and sphingo-sylphosphorylcholine [19]. Their activities are also subjected to negative regulation by specific subsets of GTPases (RhoE, Gem, Rad) [20,21] and cell cycle inhibitors ($p21^{Cip1}$) [22].

Rock proteins induce intracellular pathways that mediate the formation of stress fibres and focal adhesions, thereby participating in cell-to-cell and cell-to-substratum adhesion, cell migration and motility, phagocytosis and neurite retraction [16,17]. They also work in cell division and cytokinesis processes by regulating centrosomal functions and actomyosin ring contraction, respectively [16,17]. Deregulated signalling outputs from these kinases appear to be important for some pathologies, such as hypertension, Alzheimer's disease and cancer [12,14–17]. Demonstrating the role of these proteins in these diseases, it has been shown that the use of chemical inhibitors for Rock proteins alleviates cardiovascular pathologies such as pulmonary hypertension, vasospasms and angina pectoris [14,16,17]. Rock inhibitors also block tumorigenesis *in vitro* [23] and appear to be potentially useful for the treatment of other medical conditions including Alzheimer's disease, stroke and neuropathic pain [17].

Several Rock downstream targets have been identified, including regulators of the F-actin cytoskeleton (myosin light chain (MLC), the MLC phosphatase, Lim kinases 1 and 2), intermediate filament components (vimentin, glial fibrillary acidic protein and neurofilaments) and microtubule-associated proteins (Tau, microtubule-associated protein 2) [16,17]. Whereas the phosphorylation of MLC and its phosphatase by Rock proteins promotes the formation of F-actin fibres, the phosphorylation of other protein classes appears to induce neurofilament disassembly and to halt microtubule polymerisation. Thus, the phosphoproteome induced by Rock proteins is fully consistent with the assigned roles of these proteins in cell migration and morphology [16,17].

Similar to other serine/threonine kinases involved in signal transduction (i.e., Erk, $p38^{MAPK}$), it is possible that Rock could also promote the long-term regulation of gene expression. Consistent with this view, it has been shown that Rock activity is important for the stimulation of c-Myc by the constitutively active, oncogenic version of RhoA (Q63L mutant) [24,25] and for the expression of a small subset of the transcriptome of NIH3T3 cells transformed by the chronic expression of the *rhoA* oncogene [24]. Other studies have also shown that the expression of specific $RhoA^{Q63L}$-dependent genes is abrogated upon inhibition of the Rock pathway [26,27]. In the present study, we aimed at expanding these results to non-transformed fibroblasts. To this end, we used microarray technology to assess the effect of Y27632, a chemical inhibitor commonly used to block Rock kinase activity [28], in the transcriptome of exponentially growing NIH3T3 cells. This cell line has been widely utilised before for the characterisation of the biological properties of both Rho and Rock proteins. Previous observations by us and others have shown that Y27632 treatments inhibit several Rock-

dependent responses in this cell line, including MLC phosphorylation and stress fibre formation [23,24]. We report here the results obtained from this research avenue.

Materials and methods

Cell lines

Murine NIH3T3 cells were grown under standard temperature/CO_2 conditions in Dulbecco's modified Eagle's medium supplemented with 1% L-glutamine, 1% penicillin/streptomycin and 10% calf serum. All tissue culture reagents were obtained from Invitrogen. When appropriate, cells were treated for 24 h with 10 μM Y27632 (Cal-biochem) to inhibit endogenous Rock proteins. RhoA-transformed cells have been described before [24]. To confirm the effectiveness of Rock inactivation in this experimental setting, parallel cultures of NIH3T3 and RhoA-transformed cells were analysed by immunoblot and immunofluorescence techniques to corroborate the expected inhibition of the phosphorylation of the myosin light chain and the disassembly of stress F-actin fibres in Y27632-treated cells, as indicated and shown before [24].

Microarray experiments and data analysis

Microarray analyses were performed using RNAs obtained from seven and five independent experiments of untreated and Y27632-treated NIH3T3 cells, respectively. In each independent experiment, three 10-cm diameter plates containing exponentially growing cultures were used to generate the total RNA used in the microarray studies. To this end, cultured cells were washed with phosphate-buffered saline solution and total cellular RNAs isolated using the RNeasy kit (Qiagen) according to the supplier's specifications. The quantity and quality of the total RNAs obtained were determined using 6000 Nano Chips (Agilent Technologies). Total RNA samples (4 μg) were then processed for hybridisation on MGU75Av2 microarrays (Affymetrix) using standard Affymetrix protocols at the CIC Genomics and Proteomics Facility. Normalisation, filtering and analysis of the raw data obtained from microarrays were carried out with the Bioconductor software (www.bioconductor.com) using the *ReadAffy* package and the RMA application. We considered a gene to be differentially expressed when exhibiting a signal ≥ 100 and its fold change respect to the levels of expression of untreated NIH3T3 cells was $\geq \pm 1.5$ and with p values ≤ 0.01. Statistical analyses were performed using F-statistics.

For the graphical presentation of microarray data, we performed hierarchical clustering analysis using the WP-GA average-linkage and the standard correlation similarity metric method with the J-Express application. Functional annotation of gene functions was performed manually using internet-available databases such as those maintained by the NCBI (www.ncbi.nlm.nih.gov/sites/entrez?db=omim) and the Weizman Institute of Science (Rehovot, Israel; www.genecards.org). The identification of interactive networks of proteins and common functions was done using the Ingenuity Pathways Analysis program, a web-delivered application that enables discovery, visualisation and exploration of biological interaction networks and biological processes (www.ingenuity.com) [29]. In this case, we considered a network as significant when it fulfilled the following criteria: (i) a minimal score of 15; (ii) at least 10 proteins participating in direct, functional interactions inside the network. In addition, and to reinforce the strength of the functional relationships, we only took into consideration direct, not indirect, relationships among the network components. Bioinformatically identified networks were edited manually to sieve out proteins that, according to published data, did not have a coherent or well defined functional relationship with the other network components.

The comparison of transcriptomes between Y27632-treated non-transformed and $RhoA^{Q63L}$-transformed NIH3T3 cells was done using the previously published data on the $RhoA^{Q63L}$-dependent transcriptome [24].

Real-time quantitative RT-PCR

Exponentially growing cells treated and non-treated with Y27632 were lysed and total RNA extracted using the RNAeasy kit (Qiagen). RNAs were quantified by loading aliquots into 6000 Nano Chips. Quantitative polynucleotide chain reactions were performed using the Quanti-Tect SYBR Green RT-PCR kit (Qiagen). 18S rRNA primers were used as controls for both loading and quantitation of relative expression levels of the genes tested. Amplifications were performed using the iCycler machine (Bio-Rad). Raw data were analysed using the iCycler iQ Optical System software (version 3.0a, Bio-Rad). In other cases, quantitative RT-PCR experiments were conducted using a microfluidic card (Applied Biosystems) service available at the Program for Genomics, Proteomics and Bioinformatics of the Spanish Network of Cancer Groups.

Results and discussion

We made use of Affymetrix microarray technology to identify the transcriptomal changes induced by culturing exponentially growing NIH3T3 cells with the Rock inhibitor Y27632 for 24 h. The reason for selecting this time point was two-fold. On the one hand, it ensured effective Rock inhibition, since the dephosphorylation of MLC is detected already 6 h after addition of Y27632 and remains at low levels thereafter [24]. On the other hand, this early time point allowed us to select for primary Rock transcriptional targets rather than detecting secondary transcriptomal changes derived from the deregulation of the expression of putative Rock-dependent transcriptional factors. We also cultured cells in the presence of serum and under non-confluent conditions (approx. 70% confluency) to avoid the activation of strong genetic programs related to serum withdrawal or contact inhibition that may obscure the detection of the Rock-dependent transcriptome [30]. In addition, we isolated total RNAs from seven (in the case of NIH3T3 cells) and five (in the case of Y27632-treated cells) independent cell cultures in order to make a robust statistical treatment of the data generated possible. Total RNAs samples obtained under those conditions were converted into biotinylated-cRNA probes and hybridised independently to Affymetrix Genechip MG U74Av2 arrays, thus allowing the monitoring of the expression status of ≈12,500 mouse genes.

The results from these microarray experiments indicated that the chemical inhibition of Rock led to changes in approximately 2.3% (289 genes) of all genes probed in the arrays (Fig. 1A, B and Table 1). Interestingly, these changes involved mostly the downregulation of transcriptionally active genes (76.1% of all responsive genes), indicating that Rock activity is required primarily to maintain transcription from specific gene subsets in mouse fibroblasts. Instead, the inhibition of Rock determined the activation of a much smaller group of 69 genes. To confirm the microarray results, the expression of seven of the upregulated and ten of the downregulated genes was re-evaluated using real-time quantitative RT-PCR analysis. These analyses confirmed that these 17 genes were indeed Rock-dependent (Fig. 2). Interestingly, we also detected genes identified as Rock targets such as *cyr61, c-myc* and *cyclin D1* [24,26, 27], further supporting the validity of our microarray data.

We observed that the Rock-dependent genes were distributed following a Poisson-like distribution when classified in terms of overall fold-change variations (Fig. 1C). Thus, the majority of up- and downregulated genes displayed modest changes (1.5–2.1-fold) when their expression levels were compared between Y27632-treated and untreated NIH3T3 cells. Instead, only a small minority of genes showed fold-change variations outside that interval (Fig. 1C). Upregulated and downregulated genes followed similar trends, although we only

observed upregulated loci in the subset of genes displaying variations larger than 6-fold (Fig. 1C). We observed that the genes undergoing the largest upregulation encoded either chemokines (Ccl13, Cxcl6, Ccl7) or secreted factors (Cp and the component 3 of the complement) (Table 1). Instead, the genes with largest repressions encoded for cytoskeletal-related proteins such as actin α2, Ptx3, Thbs1 and Ogn (Table 1).

To establish an overview of the transcriptional changes induced by Rock inhibition, we assigned the 289 identified genes regulated by Y27632 to 19 different functional groups using manual annotation procedures (Fig. 3A, Table 1). This analysis revealed that the main functional groups targeted by the Y27632 include those corresponding to extra-cellular matrix proteins, membrane-localised proteins, cytoskeleton, transcriptional regulation and metabolism. With the exception of the apoptosis and cell cycle-related class, all the other functional groups contain a larger number of downregulated than of upregulated genes. In fact, five of those classes (growth factors, protein biosynthesis, heat shock, metabolism, cytoplasmic/nuclear transport) contain only repressed genes (Fig. 3A, Table 1). Interestingly, the largest percentage of upregulated genes is seen in the immune-related (83%), cell cycle (63%), ligand (58%) and membrane receptor (83%) subclasses (Table 1).

The main problem with functional annotation is that it groups genes according to functional similarity or relatedness. Due to this, this type of analysis usually oversees other important biological information, such as the interconnectivities established among genes of different functional classes, homogeneous alterations of signal transduction pathways, etc. To surmount this problem, we subjected our microarray data to further bioinformatic characterisation using the Ingenuity program. This web-based software allows the identification of common biological processes and molecular networks because it relates each gene entry with a comprehensive database of known protein–protein, transcriptional or enzymatic relationships available for = 10,000 mammalian proteins [29]. At the level of molecular networks, the analysis of the Y27632-targeted transcriptome using this bioinformatics package indicated changes in the expression of genes whose protein products are involved in integrin and c-Myc function (Fig. 3C,D). The composition of the first network is, however, limited to specific integrin subunits and proximal cytoskeletal components (see below), indicating that the signalling cascades located down-stream of integrins are not touched by the inhibition of the Rock route. The detection of the c-Myc network is of interest, because we have shown before that the overexpression of $RhoA^{Q63L}$ promotes this network whereas the inhibition of Rock downmodulates it in *rhoA*-transformed cells [24]. A third molecular network contained a larger number of protein constituents (30 in total) (Fig. 3B). This network can be further subdivided into two main branches, one that is loosely related with the Ccl7 and Ccl13 chemokines and one of its repressors (the transcriptional factor Bcl6) and another branch connecting the downmodulation of specific nuclear proteins (Xbp1, Nr2f2) with the repression of the expression of extracellular proteins such as collagen, serpin and a lipoprotein lipase (Lpl). Unlike the other two networks, this third molecular conglomerate does include nuclear, cytosolic, membrane and extracellular-located molecules, suggesting that its targeting by the Rock pathway may have some signalling purpose. To our knowledge, however, this network has not been linked to any established biological process so far. Quantitative RT-PCR experiments demonstrated that the selected elements of these three networks are indeed deregulated upon treatment of NIH3T3 cells with the Rock inhibitor (Fig. 4). At the level of biological processes affected, the bioinformatic analysis indicated that the inactivation of Rock by Y27632 alters, in a statistically significant manner ($p \leq 0.001$), genes whose protein products are primarily in charge of cellular functions usually regulated by these serine/threonine kinases such as cellular movement (migration, chemotaxis, transmigration, haptotaxis, invasion, scattering), cell morphology and the extracellular matrix. The products of these genes were also either directly (i.e., c-Myc) or indirectly (rest of genes) linked to cell growth and survival processes. However, this latter functional category probably has poor significance from a

biological point of view, because we have not detected a large pool of genes directly activated or repressed in proliferating cells (i.e., proteins directly involved in the cell cycle machinery, replication origins, DNA synthesis, etc.) (Table 1). This is consistent with previous observations by us and others indicating that Y27632 treatments do not significantly alter the proliferation rates of fibroblasts [23,24]. Based on these results, the only obvious common feature observed among these transcriptomal changes is their relationship, direct or indirect, with integral and regulatory components of cellular components usually regulated by Rock proteins such as F-actin cytoskeleton, microtubules and cell movement-related processes. Consistent with this view, it was observed that cytoskeleton-related proteins (actinin, vinculin, calponin, talin, spectrins, actin itself), cytoskeletal regulators (thy-mosin β4, myosin subunits, integrins, transgelin, catenin, Nap125, dynamin, caveolin) and microtubule-related molecules (Macf1, kinesins) showed up in most of the networks and pathways picked up by the Ingenuity software.

We have previously shown that the inhibition of Rock in $RhoA^{Q63L}$-transformed NIH3T3 cells with Y27632 also provokes minor changes in the cell transcriptome of these oncogenically transformed cells [24]. The similarity in the experimental conditions used in that work and in the current study made it possible to compare side by side the effects of Y27632 in transformed and non-transformed cells. This analysis indicated that Y27632 induced larger expression changes in the transcriptome of non-transformed (298 genes) than in $RhoA^{Q63L}$-transformed (179 genes) cells. Moreover, we have observed that the gene subsets targeted by the Rock inhibitor in the parental and the $RhoA^{Q63L}$-transformed NIH3T3 cells were significantly different, since these two transcriptomes only show 70 coincident target genes. These shared genes showed the same change pattern and belonged to both the upregulated (17 genes) and downregulated (53 genes) classes. This subset of genes included the c-Myc network detected in the Ingenuity analysis, although this interactive molecular network has a larger number of components in RhoA-transformed cells than in the non-transformed parental cells [this work, 24]. Four additional genes, although targeted by Y27632 in both cell types, showed opposite change patterns in normal and $RhoA^{Q63L}$-transformed cells. The functional classes deregulated by the Y27632 treatment that displayed more disparity between non-transformed and transformed cells were those related with membrane-located, cell adhesion-related proteins, cell cycle, DNA replication and electron transporter. The classes showing more coincident expression changes encompassed those related to extracellular, cell-adhesion-related functions, extracellular ligands, cytoskeleton, regulation of transcription and proteins with unassigned functions. These data indicate that the impact of the Rock pathway on the transcriptome is always small regardless of whether fibroblasts have normal or exacerbated RhoA activity levels. However, the type of genes targeted by this signalling route is significantly different depending on the transformed status of these cells.

In summary, these results indicate that the Rock pathway has a rather weak impact in the transcriptome of normal fibroblasts. Therefore, they are consistent with the idea that the main signalling purpose of this route is to induce phosphoproteomal rather than transcriptomal changes in the cell. Furthermore, the relative small fold change variations found in the majority of Y27632-targeted genes indicated that the transcriptional action of the Rock pathway relies mainly on modulating the levels of activity of already active genes rather than on turning on previously silent loci or turning off active genes. Interestingly, most Rock-dependent transcriptional targets are downmodulated upon inhibition of Rock activity, indicating that the Rock pathway is oriented fundamentally to the upregulation of genes under exponentially growing conditions. Finally, we have observed that the main transcriptional targets affected by the blockage of Rock activity in fibroblasts are related with processes of cell movement, cell shape and F-actin dynamics. Thus, the post-transcriptional action of Rock proteins on the F-actin cytoskeleton appears to be coordinated, in the long-term, with the modulation at the transcriptional level of genes involved in the regulation of those components of the cell

architecture. It will be important in the future to complement these studies with others focused on the cell proteome and phosphoproteome to get a comprehensive view of the effects and impact of Rock function in the biology of the mammalian cells.

Acknowledgements

We wish to thank E. Fermiñán (CIC Genomics and Proteomics Unit) and M. Blázquez for array hybridisations and general technical assistance, respectively. This work was supported by aids to XRB from the Ramón Areces Foundation, the Special Action on Genomics and Proteomics of the Spanish Ministry of Education and Science (GEN2003-20239-C06-01), the US National Cancer Institute/NIH (5R01-CA73735-11), the Spanish Ministry of Education and Science (SAF2006-01789), the Castilla-León Autonomous Government (SA053A05) and the Red Temática de Investigación Co-operativa en Cáncer (RTICC) (RD06/0020/0001, Fondo de Investigaciones Sanitarias (FIS), Carlos III Institute, Spanish Ministry of Health). IMB was supported by a FPU fellowship (FP2000-6489) of the Spanish Ministry of Education and Science and by the US National Cancer Institute. All Spanish funding is co-sponsored by the European Union FEDER programme.

References

1. Bustelo XR, Sauzeau V, Berenjeno IM. GTP-binding proteins of the Rho/Rac family: regulation, effectors and functions in vivo. Bioessays 2007 Apr;29:356–370. [PubMed: 17373658]
2. Van Aelst L, D'Souza-Schorey C. Rho GTPases and signaling networks. Genes Dev 1997;11:2295–2322. [PubMed: 9308960]
3. Symons M, Rusk N. Control of vesicular trafficking by Rho GTPases. Curr Biol 2003;13:R409–R418. [PubMed: 12747855]
4. Etienne-Manneville S, Hall A. Rho GTPases in cell biology. Nature 2002;420:629–635. [PubMed: 12478284]
5. Coleman ML, Marshall CJ, Olson MF. RAS and RHO GTPases in G1-phase cell-cycle regulation. Nat Rev Mol Cell Biol 2004;5:355–366. [PubMed: 15122349]
6. Jaffe AB, Hall A. Rho GTPases: biochemistry and biology. Annu Rev Cell Dev Biol 2005;21:247–269. [PubMed: 16212495]
7. Colicelli J. Human RAS superfamily proteins and related GTPases (250)RE13. 2004
8. DerMardirossian C, Bokoch GM. GDIs: central regulatory molecules in Rho GTPase activation. Trends Cell Biol 2005;15:356–363. [PubMed: 15921909]
9. Dransart E, Olofsson B, Cherfils J. RhoGDIs revisited: novel roles in Rho regulation. Traffic 2005;6:957–966. [PubMed: 16190977]
10. Rossman KL, Der CJ, Sondek J. GEF means go: turning on RHO GTPases with guanine nucleotide-exchange factors. Nat Rev Mol Cell Biol 2005;6:167–180. [PubMed: 15688002]
11. Bos JL, Rehmann H, Wittinghofer A. GEFs and GAPs: critical elements in the control of small G proteins. Cell 2007;129:865–877. [PubMed: 17540168]
12. Benitah SA, Valeron PF, van Aelst L, Marshall CJ, Lacal JC. Rho GTPases in human cancer: an unresolved link to upstream and downstream transcriptional regulation. Biochim Biophys Acta 2004;1705:121–132. [PubMed: 15588766]
13. Boettner B, Van Aelst L. The role of Rho GTPases in disease development. Gene 2002;286:155–174. [PubMed: 11943472]
14. Budzyn K, Marley PD, Sobey CG. Targeting Rho and Rho-kinase in the treatment of cardiovascular disease. Trends Pharmacol Sci 2002;27:97–104. [PubMed: 16376997]
15. Sahai E, Marshall CJ. RHO-GTPases and cancer. Nat Rev Cancer 2002;2:133–142. [PubMed: 12635176]
16. Riento K, Ridley AJ. Rocks: multifunctional kinases in cell behaviour. Nat. Rev. Cell Biol 2003;4:446–456.
17. Mueller BK, Mack H, Teusch N. Rho kinase, a promising drug target for neurological disorders. Nat Rev Drug Discov 2005;4:387–398. [PubMed: 15864268]
18. Fu X, Gong MC, Jia T, Somlyo AV, Somlyo AP. The effects of the Rho-kinase inhibitor Y-27632 on arachidonic acid-, GTPgammaS-, and phorbol ester- induced Ca2+-sensitization of smooth muscle. FEBS Lett 1998;440:183–187. [PubMed: 9862451]

19. Shirao S, Kashiwagi S, Sato M, et al. Sphingosylphosphorylcholine is a novel messenger for Rho-kinase-mediated Ca2+ sensitization in the bovine cerebral artery: unimportant role for protein kinase C. Circulation research 2002;91:112–119. [PubMed: 12142343]

20. Riento K, Guasch RM, Garg R, Jin B, Ridley AJ. RhoE binds to ROCK I and inhibits downstream signaling. Mol Cell Biol 2003;23:4219–4229. [PubMed: 12773565]

21. Ward Y, Yap SF, Ravichandran V, Matsumura F, Ito M, Spinelli B, Kelly K. The GTP binding proteins Gem and Rad are negative regulators of the Rho-Rho kinase pathway. J Cell Biol 2002;157:291–302. [PubMed: 11956230]

22. Lee S, Helfman DM. Cytoplasmic p21Cip1 is involved in Ras-induced inhibition of the ROCK/LIMK/cofilin pathway. J Biol Chem 2004;279:1885–1891. [PubMed: 14559914]

23. Sahai E, Ishizaki T, Narumiya S, Treisman R. Transformation mediated by RhoA requires activity of ROCK kinases. Curr Biol 1999;9:136–145. [PubMed: 10021386]

24. Berenjeno IM, Nunez F, Bustelo XR. Transcriptomal profiling of the cellular transformation induced by Rho subfamily GTPases. Oncogene 2007;26:4295–4305. [PubMed: 17213802]

25. Chiariello M, Marinissen MJ, Gutkind JS. Regulation of c-myc expression by PDGF through Rho GTPases. Nat Cell Biol 2001;3:580–586. [PubMed: 11389443]

26. Han JS, Macarak E, Rosenbloom J, Chung KC, Chaqour B. Regulation of Cyr61/CCN1 gene expression through RhoA GTPase and p38MAPK signaling pathways. Eur J Biochem 2003;270:3408–3421. [PubMed: 12899698]

27. Croft DR, Olson MF. The Rho GTPase effector ROCK regulates cyclin A, cyclin D1, and p27Kip1 levels by distinct mechanisms. Mol Cell Biol 2006;26:4612–4627. [PubMed: 16738326]

28. Uehata M, Ishizaki T, Satoh H, et al. Calcium sensitization of smooth muscle mediated by a Rho-associated protein kinase in hypertension. Nature 1997;389:990–994. [PubMed: 9353125]

29. Calvano SE, Xiao W, Richards DR, et al. A network-based analysis of systemic inflammation in humans. Nature 2005 Oct 13;437(7061):1032–1037. [PubMed: 16136080]

30. Coller HA, Sang L, Roberts JM. A new description of cellular quiescence. PLoS Biol 2006;4:e83. [PubMed: 16509772]

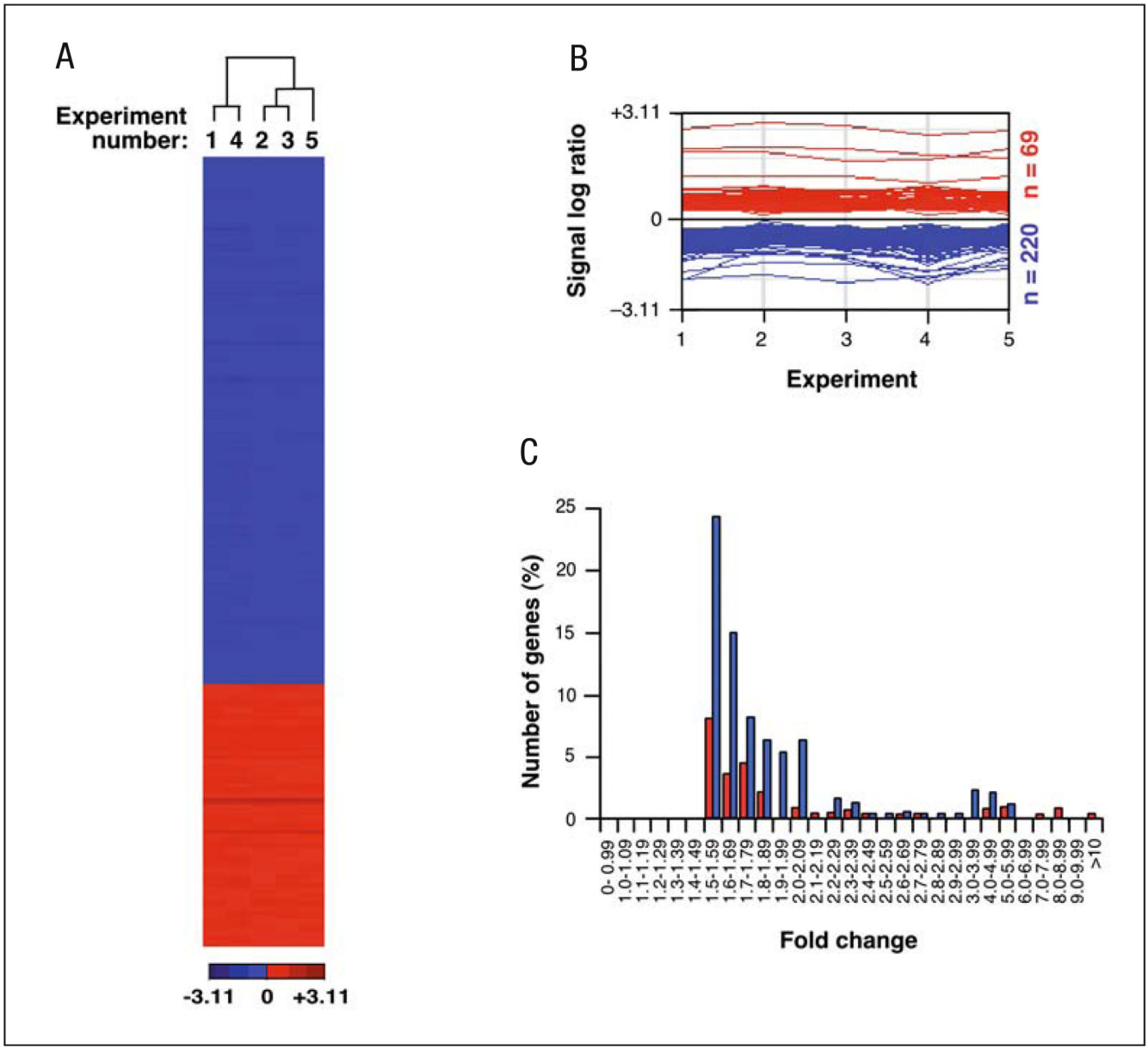

Fig. 1.

Transcriptomal changes induced by Y27632 in exponentially growing NIH3T3 cells. **A** Hierarchical cluster diagram of the 289 genes whose expression levels changed in Y27632-treated cells. Each column represents one experiment and each row a gene. Varying levels of expression are represented on a scale from dark blue (lowest expression) to dark red (highest expression). Note that expression values are represented as signal log ratio numbers (SLR) and that, therefore, the total fold change value is obtained from 2^{SLR}. The experiment number is shown at the top of each column. **B** Gene graphs showing the induced (red) and repressed (blue) genes in Y27632-treated cells. In each category, the expression values of all deregulated genes are represented as SLR (considering that fold change is 2^{SLR}; *y*-axis) obtained in each experimental sample (*x*-axis). The total number of upregulated and downregulated genes in each category is indicated on the right of each panel. **C** Histogram showing the number of up-

(red) and downregulated (blue) genes with a given expression fold change value in Y27632-treated cells

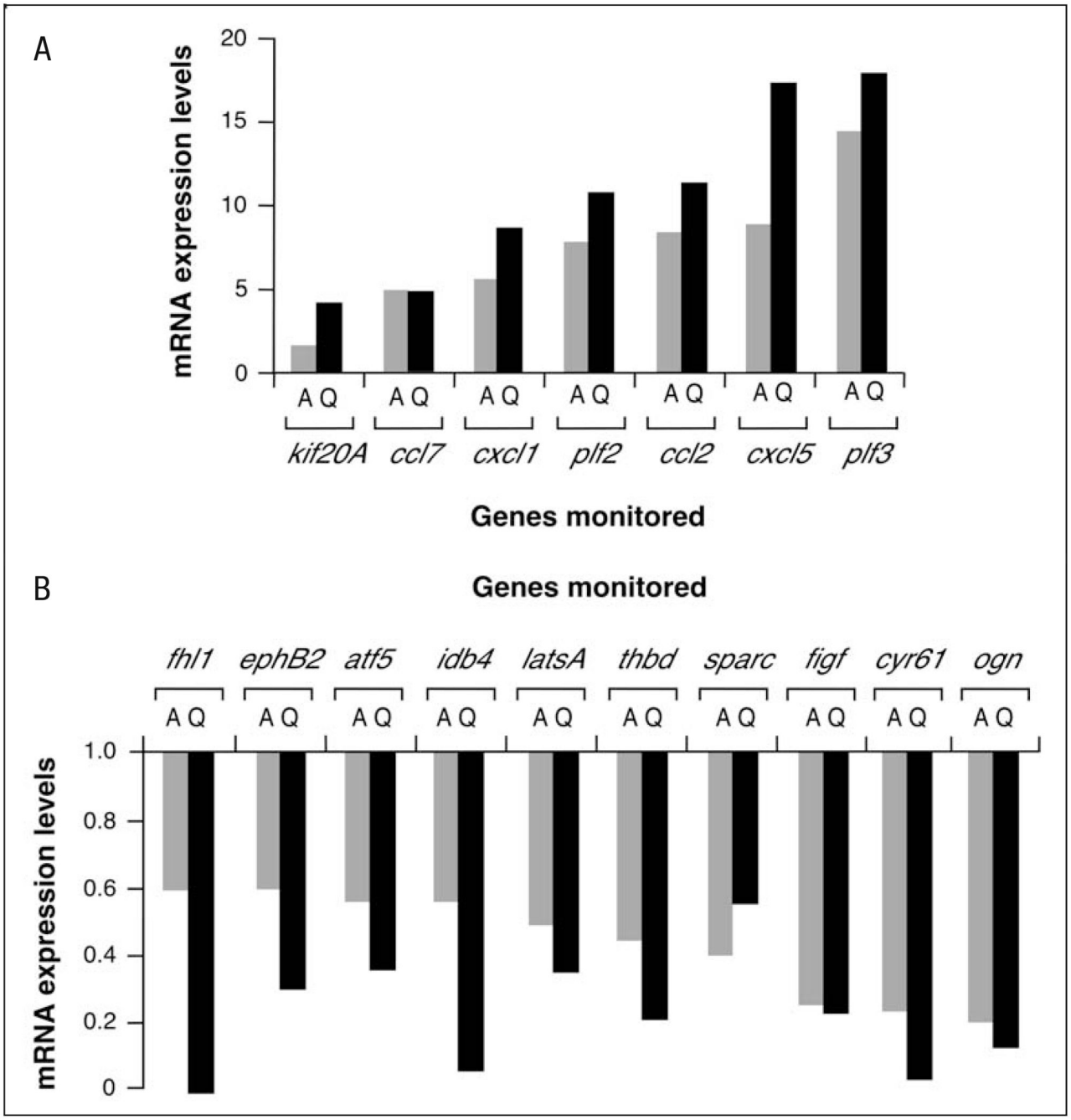

Fig. 2.

Corroboration of Affymetrix data by quantitative RT-PCR. **A, B** Expression levels of the indicated up-regulated (A) and downregulated (B) mRNAs by the Y27632 treatment were determined by either microarray (A, grey bars) or quantitative RT-PCR (Q, black bars). Values are expressed as fold change of the appropriate gene with respect to the transcript levels found in untreated NIH3T3 cells

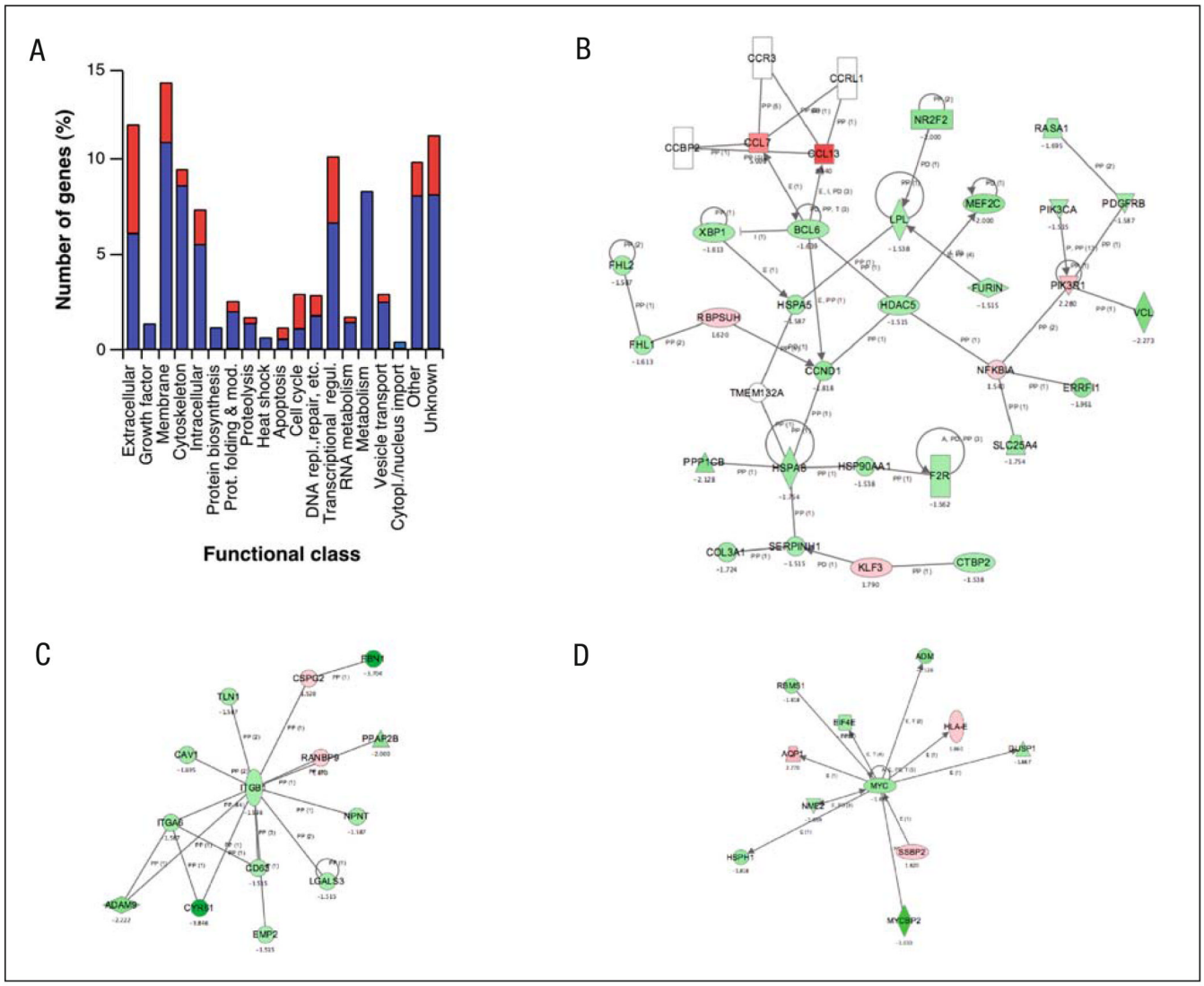

Fig. 3.

Functional annotation and characterisation of Y27632-dependent genes. **A** Classification of up- (red) and downregulated (blue) genes by the Y27632 treatment according to general biological functions. **B**–**D** The molecular networks identified using the Ingenuity database in the Y27632-affected transcriptome. Nodes are colour-coded in red (upregulated) or green (downregulated) according to their fold change values

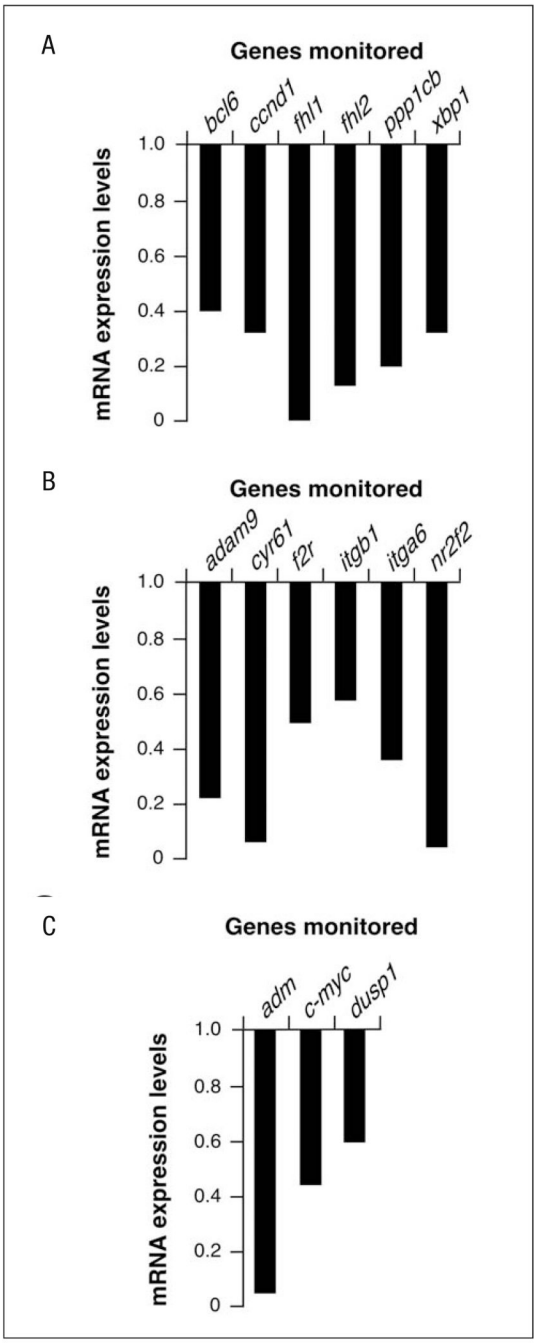

Fig. 4.

Corroboration of the molecular networks identified in Fig. 3 by quantitative RT-PCR. **A**–**C** RT-PCR-determined expression levels of selected genes belonging to the molecular networks shown in Fig. 3B (A), 3C (B) and 3D (C). Values are expressed as fold change of the appropriate gene with respect to the transcript levels found in untreated NIH3T3 cells

Clin Transl Oncol. Author manuscript; available in PMC 2009 September 4.

Table 1

List of genes whose expression is upregulated or downregulated by Y27632 in NIH3T3 cells[a]

Function	Locus ID	Gene	Description	Change[b]	*p* value[c]
Extracellular					
Cell adhesion	12825	Col3a1	Procollagen, type III, alpha 1	0.58	0.0017
	12832	Col5a2	Procollagen, type V, alpha 2	0.55	0.0001
	13003	Cspg2	Chondroitin sulfate proteoglycan 2	1.52	<1.00E-04
	16007	Cyr61	Cysteine-rich protein 61	0.26	0.0001
	16779	Lamb2	Laminin, beta 2	0.52	0.0014
	17313	Mglap	Matrix gamma-carboxyglutamate protein	0.53	<1.00E-04
	17395	Mmp9	Matrix metalloproteinase 9	1.5	<1.00E-04
	114249	Npnt	Mus musculus transcribed sequences	0.63	0.0001
	18787	Serpine1	Serine (or cysteine) proteinase inhibitor 1	0.61	0.0074
	20720	Serpine2	Serine (or cysteine) proteinase inhibitor, 2	0.38	0.0001
	20692	Sparc	Secreted acidic cysteine rich glycoprotein	0.41	<1.00E-04
	13602	Sparcl1	SPARC-like 1	1.54	0.0095
	21810	Tgfbi	Transforming growth factor beta induced	1.57	<1.00E-04
Immune response	12266	C3	Complement component 3	4.55	<1.00E-04
	19288	Ptx3	Pentaxin related gene	0.21	<1.00E-04
	20568	Slpi	Secretory leukocyte protease inhibitor	2.39	<1.00E-04
	20210	Saa3	Serum amyloid A3	1.89	<1.00E-04
Ion transport	12870	Cp	Ceruloplasmin	4.77	<1.00E-04
Ligand	14824	Grn	Granulin	0.66	0.0039
	23893	Grem2	Gremlin 2 homolog	1.76	0.001
	20750	Spp1	Secreted phosphoprotein 1	1.82	0.0017
	18812	Plf2	Proliferin 2	7.7	<1.00E-04
	20311	Cxcl5	Chemokine (C-X-C motif) ligand 5	8.83	<1.00E-04
	11535	Adm	Adrenomedullin	0.47	<1.00E-04
	13642q	Efnb2	Ephrin B2	0.61	0.0068
	20306	Ccl7	Chemokine (C-C motif) ligand 7	5	<1.00E-04
	14825	Cxcl1	Chemokine (C-X-C motif) ligand 1	5.56	<1.00E-04
	20296	Ccl2	Chemokine (C-C motif) ligand 2	8.34	<1.00E-04
	26421	Mrpplf3	Proliferin 3	14.29	<1.00E-04

Function	Locus ID	Gene	Description	Change[b]	*p* value[c]
	21825	Thbs1	Thrombospondin 1	0.21	<1.00E-04
Other	14118	Fbn1	Fibrillin 1	0.65	0.0064
	50530	Mfap5	Microfibrillar associated protein 5	0.5	0.0023
	18451	P4ha1	Procollagen-proline, 2-oxoglutarate 4-dioxygenase a 1	0.64	<1.00E-04
	14827	Pdia3	Protein disulfide isomerase associated 3	0.48	<1.00E-04
Receptor activity	12931	Crlf1	Cytokine receptor-like factor 1	1.76	0.0004
Growth factor	12977	Csf1	Colony stimulating factor 1	0.61	<1.00E-04
	14205	Figf	C-Fos induced growth factor	0.27	0.0002
	18295	Ogn	Osteoglycin	0.22	<1.00E-04
	19242	Ptn	Pleiotrophin	0.31	0.0015
Membrane					
Cell adhesion	12558	Cdh2	Cadherin 2	0.47	<1.00E-04
	16403	Itga6	Integrin alpha 6	0.63	0.0003
Membrane/cell adhesion	20320	Sdfr1	Stromal cell derived factor receptor 1	0.63	0.0004
Channel-transporter	11826	Aqp1	Aquaporin 1	2.77	<1.00E-04
	14726	Gp38	Glycoprotein 38	0.57	0.0001
	16497	Kcnab1	Potassium voltage-gated channel beta member 1	0.66	0.0011
	20514	Slc1a7	Solute carrier family 1, member 7	0.45	0.0001
	67760	Slc38a2	Solute carrier family 38, member 2	0.52	0.0004
	22334	Vdac2	Voltage-dependent anion channel 2	0.57	<1.00E-04
Immune response	15040	H2-T23	Histocompatibility 2, T region locus 23	1.86	0.0008
	17069	Ly6e	Lymphocyte antigen 6 complex, locus E	1.57	<1.00E-04
Receptor activity	11609	Agtr2	Angiotensin II receptor, type 2	0.43	0.0026
	14062	F2r	Coagulation factor II (thrombin) receptor	0.64	<1.00E-04
	20321	Frrs1	Ferric-chelate reductase 1	0.6	0.0003
	83924	Gpr137b	G protein-coupled receptor 137B	2.39	<1.00E-04
	16412	Itgb1	Integrin beta 1	0.65	0.0003
	16948	Lox	Lysyl oxidase	0.66	0.0003
	16974	Lrp6	Low density lipoprotein receptor-related protein 6	0.64	0.0012
	319900	Npr3	Natriuretic peptide receptor 3	0.33	0.0011
	18186	Nrp	Neuropilin	0.4	<1.00E-04

Function	Locus ID	Gene	Description	Change[b]	*p* value[c]
	19220	Ptgfr	Prostaglandin F receptor	2.44	<1.00E-04
	21824	Thbd	Thrombomodulin	0.47	0.0001
	18383	Tnfrsf11b	Tumour necrosis factor receptor superfamily 1b	1.57	0.0007
	21937	Tnfrsf1a	Tumour necrosis factor receptor superfamily 1a	1.52	0.0015
	14102	Tnfrsf6	Tumour necrosis factor receptor superfamily 6	1.57	<1.00E-04
Signal transducer activity	11487	Adam10	A disintegrin and metalloprotease domain 10	0.62	0.0004
	17118	Marcks	Myristoylated alanine rich protein kinase C substrate	0.42	0.0001
	18858	Pmp22	Peripheral myelin protein	0.64	0.0007
	20338	Sel1h	Sel1 1 homolog	0.52	<1.00E-04
Other	11502	Adam9	A disintegrin and metalloproteinase domain 9	0.45	<1.00E-04
	319434	Amot	Angiomotin	0.6	
	13244	Degs	Degenerative spermatocyte homologue	0.57	<1.00E-04
	53872	Gpiap1	GPI-anchored membrane protein 1	0.58	0.0005
	20014	Rpn2	Ribophorin II	0.64	0.0033
	20324	Sdpr	Serum deprivation response	0.37	<1.00E-04
	20908	Stx3	Syntaxin 3	0.53	0.0014
	21838	Thy1	Thymus cell antigen 1 theta	0.5	<1.00E-04
	232086	TM6P1	Fasting-inducible integral membrane protein TM6P1	0.65	0.0094
Nuclear membrane	67154	Mtdh	Metadherin	0.65	0.0063
Cytoskeleton	226251	Ablim1	Actin-binding LIM protein 1	0.56	0.0023
	26357	Abcg2	ATP-binding cassette, sub-family G2	0.65	0.0023
	11475	Acta2	Actin, alpha 2, smooth muscle	0.18	<1.00E-04
	11464	Actc1	Actin, alpha, cardiac	0.57	<1.00E-04
	109711	Actn1	Actinin alpha 1	0.54	0.0008
	12798	Cnn2	Calponin 2	0.49	<1.00E-04
	13007	Csrp1	Cysteine and glycine-rich protein 1	0.58	0.0001
	13860	Eps8	Epidermal growth factor receptor pathway substrate 8	0.56	0.0001
	14086	Fscn1	Fascin homologue 1	0.55	<1.00E-04
	56486	Gabarap	Gamma-aminobutyric acid receptor associated protein	0.66	0.0004
	19348	Kif20a	Kinesin family member 20A	1.64	0.0049
	16571	Kif4	Kinesin family member 4	1.89	0.007

Function	Locus ID	Gene	Description	Change[b]	*p* value[c]
	16573	Kif5b	Kinesin family member 5B	0.57	0.0014
	65970	Lima1	LIM domain and actin binding 1	0.61	0.0009
	11426	Macf1	Microtubule-actin crosslinking factor 1	0.64	< 1.00E-04
	17886	Myh9	Myosin heavy chain IX	0.49	<1.00E-04
	17909	Myo10	Myosin X	0.6	0.0002
	83431	Ndel1	Nuclear distribution gene E-like homolog 1	0.63	0.0001
	218952	Plekhc1	Pleckstrin homology domain containing, family C1	0.56	0.0001
	20740	Spna2	Spectrin alpha 2	0.49	0.0004
	20742	Spnb2	Spectrin beta 2	0.55	0.0005
	104027	Synpo	Synaptopodin	0.59	0.0028
	21345	Tagln	Transgelin	0.26	<1.00E-04
	21894	Tln	Talin	0.63	<1.00E-04
	19241	Tmsb4x	Thymosin, beta 4, X chromosome	0.51	<1.00E-04
	22003	Tpm1	Tropomyosin 1, alpha	0.59	<1.00E-04
	22330	Vcl	Vinculin	0.44	<1.00E-04
Intracellular					
Signal transducer activity	12388	Catns	Catenin src	0.6	0.0035
	83397	Akap12	A kinase anchor protein 12	0.38	0.0001
	54519	Apbb1ip	Amyloid beta precursor-binding 1 interacting protein	0.43	<1.00E-04
	80837	Arhj	Ras homologue gene family J	0.64	0.0046
	19252	Dusp1	Dual specificity phosphatase 1	0.6	0.0002
	67603	Dusp6	Dual specificity phosphatase 6	0.24	<1.00E-04
	74155	Errfi1	ERBB receptor feedback inhibitor 1	0.51	0.0027
	212398	Frat2	Frequently rearranged in T-cell lymphomas 2	1.57	<1.00E-04
	16413	Itgb1bp1	Integrin beta 1 binding protein 1	0.6	<1.00E-04
	50523	Lats2	Large tumour suppressor 2	0.52	0.0001
	26410	Map3k8	Mitogen activated protein kinase kinase kinase 8	1.7	<1.00E-04
	18647	Pftk1	PFTAIRE protein kinase 1	0.63	<1.00E-04
	18708	Pik3r1	P85 alpha	2.28	<1.00E-04
	19046	Ppp1cb	Protein phosphatase 1, catalytic subunit, beta isoform	0.47	0.0013
	56044	Rala	V-ral simian leukaemia viral oncogene homologue A	0.63	0.001

Function	Locus ID	Gene	Description	Change[b]	*p* value[c]
	218397	Rasa1	RAS p21 protein activator 1	0.63	0.0009
	56437	Rrad	Ras-related associated with diabetes	1.52	<1.00E-04
	16765	Stmn1	Stathmin 1	1.82	0.0077
	21353	Tank	TRAF NF-kappa B activator	0.48	0.0001
	68842	Tulp4	Tubby like protein 4	0.65	0.0012
	59043	Wsb2	WD-40-repeat-containing protein with a SOCS box	0.52	<1.00E-04
Protein biosynthesis	16341	Eif3s6	Eukaryotic translation initiation factor 3, subunit 6	0.58	0.0026
	107508	Eprs	Glutamyl-prolyl-trna synthetase	0.66	0.0052
	23874	Farsl	Phenylalanine-tRNA synthetase-like	0.65	0.003
Protein folding and modification	12469	Cct8	Chaperonin subunit 8	0.64	0.0021
	14976	H2-Ke2	H2-K region expressed gene 2	1.52	0.0015
	14828	Hspa5	Heat shock 70 kDa protein 5	0.63	0.0011
	15481	Hspa8	Heat shock protein 8	0.59	<1.00E-04
	217664	Mgat2	Mannoside acetylglucosaminyltransferase 2	0.61	0.0005
	12406	Serpinh1	Serine (or cysteine) proteinase inhibitor, clade H 1	0.66	0.0001
	54609	Ubqln2	Ubiquilin 2	0.52	0.0004
Proteolysis and peptidolysis	67526	Apg12l	Autophagy 12-like	1.73	0.0004
	17035	Lxn	Latexin	0.58	0.0069
	22194	Ube2e1	Ubiquitin-conjugating enzyme E2E 1	0.52	0.0022
	70620	Ube2v2	Ubiquitin-conjugating enzyme E2 variant 2	0.66	0.004
	59025	Usp14	Ubiquitin specific protease 14	0.62	0.0025
Heat shock	15505	Hsp105	Heat shock protein 105	0.55	<1.00E-04
	15519	Hspca	Heat shock protein 1 alpha	0.65	0.0009
Apoptosis	54673	Bif-1	SH3-domain GRB2-like B1	0.58	<1.00E-04
	12363	Casp4	Caspase 4, apoptosis-related cysteine protease	1.64	<1.00E-04
	114774	Pawr	PRKC apoptosis WT1 regulator	0.59	0.0011
Cell cycle	215387	Brrn1	Barren homologue	1.79	0.0086
	12442	Ccnb2	Cyclin B2	1.82	0.0003
	12443	Ccnd1	Cyclin D1	0.55	<1.00E-04
	12453	Ccni	Cyclin I	0.54	0.002
	12532	Cdc25c	Cell division cycle 25 homologue C	1.79	0.0054

Function	Locus ID	Gene	Description	Change[b]	*p* value[c]
	12545	Cdc7	Cell division cycle 7	1.5	0.0038
	59125	Nek7	NIMA-related expressed kinase 7	0.65	0.0001
	30939	Pttg1	Pituitary tumour-transforming 1	2	0.0002
DNA replication and repair	12615	Cenpa	Centromere autoantigen A	2	0.0007
	69072	Ebna1bp2	EBNA1 binding protein 2	0.6	0.0016
	15569	Elavl2	ELAV-like 2	0.62	0.0001
	15078	H3f3a	H3 histone, family 3A	0.58	0.0011
	15364	Hmga2	High mobility group AT-hook 2	0.66	0.0005
	15354	Hmgb3	High mobility group box 3	2.18	0.0024
	50887	Nsbp1	Nucleosome binding protein 1	1.54	0.0006
	21974	Top2b	Topoisomerase (DNA) II beta	0.63	0.0003
Regulation of transcription	107503	Atf5	Activating transcription factor 5	0.58	<1.00E-04
	12034	Bcap37	Dentatorubral pallidoluysian atrophy	1.58	0.0002
	12051	Bcl3	B-cell leukaemia/lymphoma 3	1.59	<1.00E-04
	12053	Bcl6	B-cell leukaemia/lymphoma 6	0.61	<1.00E-04
	57316	C1d	C1d nuclear DNA binding protein	0.64	0.0083
	17684	Cited2	Cbp/p300-interacting transactivator 2	0.59	<1.00E-04
	107765	Crap	Cardiac responsive adriamycin protein	0.35	<1.00E-04
	13017	Ctbp2	C-terminal binding protein 2	0.65	0.001
	23871	Ets1	E26 avian leukemia oncogene 1	0.61	0.0054
	14200	Fhl2	Four and a half LIM domains 2	0.66	<1.00E-04
	15904	Idb4	Inhibitor of DNA binding 4	0.57	0.0003
	26388	Ifi202b	Interferon activated gene 202B	0.52	0.0002
	16978	Lrrfip1	Leucine rich repeat interacting protein 1	0.49	<1.00E-04
	17869	Myc	Myelocytomatosis oncogene	0.54	0.0055
	27057	Ncoa4	Nuclear receptor coactivator 4	0.63	0.0001
	18028	Nfib	Nuclear factor I/B	0.57	0.0031
	18035	Nfkbia	Nuclear factor of kappa B inhibitor alpha	1.7	<1.00E-04
	80859	Nfkbiz	Nuclear factor of kappa B inhibitor zeta	2.64	<1.00E-04
	353187	Nr1d2	Nuclear receptor subfamily 1, group D, member 2	1.5	0.0001
	11819	Nr2f2	Nuclear receptor subfamily 2, group F, member 2	0.5	<1.00E-04

Function	Locus ID	Gene	Description	Change[b]	*p* value[c]
	22634	Plagl1	Pleiomorphic adenoma gene-like 1	0.61	0.0093
	19664	Rbpsuh	Recombining binding protein suppressor of hairless	1.67	<1.00E-04
	19698q	Relb	Avian reticuloendotheliosis viral (v-rel) oncogene B	1.62	<1.00E-04
	67155	Smarca2	SWI/SNF related, matrix associated, actin dependent regulator of chromatin, subf.a, mem2	0.43	6.00E-04
	20677	Sox4	SRY-box containing gene 4	1.79	<1.00E-04
	21807	Tgfb1i4	Transforming growth factor beta 1 induced transcript 4	1.57	<1.00E-04
	228775	Trib3	Tribbles homologue 3	1.67	<1.00E-04
	22160	Twist1	Ubiquitin-conjugating enzyme E2D 3	0.5	<1.00E-04
	22433	Xbp1	X-box binding protein 1	0.62	<1.00E-04
RNA metabolism	14007	Cugbp2	CUG triplet repeat,RNA binding protein 2	0.52	0.0004
	18569	Pdcd4	Programmed cell death 4	0.63	0.0017
	81898	Sf3b1	Splicing factor 3b, subunit 1	0.52	0.0001
	20823	Ssb	Sjogren syndrome antigen B	0.54	0.0016
	12192	Zfp36l1	Zinc finger protein 36, C3H type-like 1	1.73	0.0001
Metabolism					
Lipid metabolism	208715	Hmgcs1	3-Hydroxy-3-methylglutaryl-Coenzyme A synthase 1	0.62	<1.00E-04
	16956	Lpl	Lipoprotein lipase	0.65	0.0017
	67041	Oxct	3-Oxoacid coa transferase	0.66	0.0001
	27273	Pdk4	Pyruvate dehydrogenase kinase, isoenzyme 4	0.63	0.0013
	18783	Pla2g4a	Phospholipase A2, group IVA	0.66	0.0008
	66234	Sc4mol	Sterol-C4-methyl oxidase-like	0.63	<1.00E-04
	235293	Sc5d	Sterol-C5-desaturase	0.47	0.0005
	20397	Sgpl1	Sphingosine phosphate lyase 1	0.66	0.0004
	56442	Tde1l	Tumour differentially expressed 2	0.63	0.0001
Carbohydrate metabolism	15926	Idh1	Isocitrate dehydrogenase 1 (NADP+)	0.64	0.0005
Nucleic acid-related	104444	Rexo2	RNA exonuclease 2 homologue	0.57	< 1.00E-04
Electron transporter	70495	Atp6ip2	Atpase, H+ transporting accessory protein 2	0.58	0.0003
	11972	Atp6v0d1	Atpase, H+ transporting, V0 subunit D isoform 1	0.59	0.0003
	11964	Atp6v1a1	Atpase, H+ transporting, V1 subunit A, isoform 1	0.53	0.0004
	11966	Atp6v1b2	Atpase, H+ transporting, V1 subunit B, isoform 2	0.62	0.0013
	66335	Atp6v1c1	Atpase, H+ transporting, V1 subunit C, isoform 1	0.63	0.0002

Function	Locus ID	Gene	Description	Change[b]	*p* value[c]
	12864	Cox6c	Cytochrome c oxidase, subunit vic	0.64	0.0003
	13078	Cyp1b1	Cytochrome P450, family 1, subfamily b, polypep. 1	0.53	0.0008
Glutathione metabolism	14873	Gsto1	Glutathione S-transferase omega 1	0.66	<1.00E-04
Other	11668	Aldh1a1	Aldehyde dehydrogenase family 1, subfamily A1	0.23	0.001
	56332	Amotl2	Angiomotin like 2	0.45	<1.00E-04
	14199	Fhl1	Four and a half LIM domains 1	0.62	0.0015
	15939	Ier5	Immediate early response 5	0.33	<1.00E-04
	17161	Maoa	Monoamine oxidase A	0.44	<1.00E-04
	19317	Qk	Quaking	0.58	0.001
	52357	Wwc2	WW, C2 and coiled-coil domain containing 2	0.61	<1.00E-04
Other	11630	Aim1	Absent in melanoma 1	1.52	0.0001
	11737	Anp32a	Acidic nuclear phosphoprotein 32 family, member A	1.5	<1.00E-04
	20239	Atxn2	Ataxin 2	0.66	<1.00E-04
	110147	Bat8	HLA-B associated transcript 8	0.65	0.0002
	223770	Brd1	Bromodomain containing 1	0.64	0.0005
	12512	Cd63	Cd63 antigen	0.66	<1.00E-04
	321022	Cdv3	Carnitine deficiency-associated of ventricle 3	0.63	0.0001
	13008	Csrp2	Cysteine and glycine-rich protein 2	1.67	0.0001
	13025	Ctla2b	Cytotoxic T lymphocyte-associated protein 2 beta	0.56	0.0077
	14209	Fin14	Fibroblast growth factor inducible 14	0.63	0.0073
	17263	Gtl2	GTL2, imprinted maternally expressed mRNA	0.65	0.0028
	72568	Lin9	Lin-9 homologue	1.54	0.0025
	17184	Matr3	Matrin 3	0.65	0.006
	17966	Nbr1	Neighbour of Brca1 gene 1	0.6	<1.00E-04
	30877	Ns	Nucleostemin	0.61	0.0003
	18203	Ntan1	N-terminal Asn amidase	0.59	0.0001
	269424	Phf17	PHD finger protein 17	0.6	0.0001
	56705	Ranbp9	RAN binding protein 9	0.6	0.0003
	26611	Rcn2	Reticulocalbin 2	0.59	0.0012
	319714	Rnase4	Ribonuclease, rnase A family 4	0.51	0.0043
	20715	Serpina3g	Serine (or cysteine) proteinase inhibitor, clade A-3G	1.64	<1.00E-04

Function	Locus ID	Gene	Description	Change[b]	*p* value[c]
	94186	Strn3	Striatin, calmodulin binding protein 3	0.52	0.0001
	22134	Tgoln1	Trans-Golgi network protein	0.63	0.0005
	53612	Vti1b	Vesicle transport t-SNARE interactor, 1B homologue	0.61	0.0001
	211652	Wwc1	WW, C2 and coiled-coil domain containing 1	0.47	<1.00E-04
	53861	Zfp265	Zinc finger protein 265	0.61	0.0055
Transport					
Vesicle transport	16952	Anxa1	Annexin A1	0.34	<1.00E-04
	11745	Anxa3	Annexin A3	0.27	<1.00E-04
	12389	Cav	Caveolin, caveolae protein	0.59	0.0001
	13429	Dnm	Dynamin	1.62	<1.00E-04
	16784	Lamp2	Lysosomal membrane glycoprotein 2	0.62	0.0002
	53869	Rab11a	RAB11a, member RAS oncogene family	0.63	0.0004
	22319	Vamp3	Vesicle-associated membrane protein 3	0.6	0.0036
Protein-nucleus import	16649	Kpna4	Karyopherin alpha 4	0.53	0.0002
Protein transport	216363	Rab3ip	RAB3A interacting protein	0.65	<1.00E-04

[a] Genes have been classified into 19 different functional groups. The locus identification number (Locus ID), the gene symbol (gene) and spelled out designation of each gene are shown. For the sake of simplicity, EST clones with unknown functions have not been included in the list.

[b] Fold change in gene expression levels upon a 24-h-long treatment with Y27632.

[c] p-values of genes affected in NIH3T3 cells determined with the F-statistic. *p*-values lower than 1.00E-04 are shown as <1.00E-04